ChemPubSoc Europe

DOI: 10.1002/chem.201901664

CHEMISTRY
A European Journal
Communication

Enzyme Inhibitors

Targeting a Large Active Site: Structure-Based Design of Nanomolar Inhibitors of *Trypanosoma brucei* Trypanothione Reductase

Raoul De Gasparo,[a] Ondrej Halgas,[b, c] Dora Harangozo,[a] Marcel Kaiser,*[d, e] Emil F. Pai,*[b, c] R. Luise Krauth-Siegel,*[f] and François Diederich*[a]

Abstract: Trypanothione reductase (TR) plays a key role in the unique redox metabolism of trypanosomatids, the causative agents of human African trypanosomiasis (HAT), Chagas' disease, and leishmaniases. Introduction of a new, lean propargylic vector to a known class of TR inhibitors resulted in the strongest reported competitive inhibitor of *Trypanosoma* (*T.*) *brucei* TR, with an inhibition constant K_i of 73 nM, which is fully selective against human glutathione reductase (hGR). The best ligands exhibited in vitro IC_{50} values (half-maximal inhibitory concentration) against the HAT pathogen, *T. brucei rhodesiense*, in the mid-nanomolar range, reaching down to 50 nM. X-Ray co-crystal structures confirmed the binding mode of the ligands and revealed the presence of a HEPES buffer molecule in the large active site. Extension of the propargylic vector, guided by structure-based design, to replace the HEPES buffer molecule should give inhibitors with low nanomolar K_i and IC_{50} values for in vivo studies.

[a] *Dr. R. De Gasparo, D. Harangozo, Prof. Dr. F. Diederich*
Laboratorium für Organische Chemie, ETH Zurich
Vladimir-Prelog-Weg 3, 8093 Zurich (Switzerland)
E-mail: diederich@org.chem.ethz.ch

[b] *O. Halgas, Prof. Dr. E. F. Pai*
Departments of Biochemistry and Medical Biophysics
University of Toronto
Medical Sciences Building, 5318, 1 King's College Circle
Toronto, ON, M5S 1A8 (Canada)
E-mail: emil.pai@utoronto.ca

[c] *O. Halgas, Prof. Dr. E. F. Pai*
The Campbell Family Institute for Cancer Research
University Health Network
101 College Street, Toronto, ON, M5G 1L7 (Canada)

[d] *Dr. M. Kaiser*
Swiss Tropical and Public Health Institute
Socinstrasse 57, 4002 Basel, (Switzerland)
E-mail: marcel.kaiser@swisstph.ch

[e] *Dr. M. Kaiser*
University of Basel
Petersplatz 1, 4003 Basel (Switzerland)

[f] *Prof. Dr. R. L. Krauth-Siegel*
Biochemie-Zentrum Heidelberg (BZH), Universität Heidelberg
Im Neuenheimer Feld 328, 69120 Heidelberg (Germany)
E-mail: luise.krauth-siegel@bzh.uni-heidelberg.de

Supporting information and the ORCID identification number(s) for the author(s) of this article can be found under: https://doi.org/10.1002/chem.201901664.

The neglected tropical diseases human African trypanosomiasis (HAT), Chagas' disease, and the different forms of leishmaniasis constitute one of the most serious health problems in developing countries, with an estimated 500 million people at risk of infection.[1] Currently used drugs have major drawbacks, such as poor safety, complicated administration, and high cost, underscoring the necessity for new, safe, and inexpensive treatments.[1b,2] Whereas virtually all other organisms have a glutathione/glutathione reductase (GR) redox system, trypanosomatids are characterized by a unique trypanothione-based thiol metabolism.[3] Trypanothione reductase (TR) plays a central role in this unique metabolism by catalyzing the reduction of trypanothione disulfide to trypanothione, which the parasites use in several essential processes, such as protection against oxidative damage.[3a] Over the last 30 years, following the discovery of TR,[4] a large number of inhibitors have been reported that target the large solvent-exposed active site of TR but typically achieved only inhibition constants (K_i) in the low micromolar range,[2a,5] far from the low nanomolar range necessary to achieve significant in vivo inhibition of TR.[5d,6]

We have recently reported[7] on a known class of TR ligands[5c,8] providing a novel lead **1** with improved potency (competitive inhibition constant (K_{ic}) = 6.1 μM) and physicochemical properties (Figure 1). The crystal structure of **1** in complex with *Trypanosoma* (*T.*) *brucei* TR confirmed binding of the inhibitor to the so-called mepacrine binding site[9] and suggested directions for further development of this ligand class[7] (see Figure S1 in the Supporting Information).

In this work, we describe the structure-based design-guided (see Section S2 in the Supporting Information) improvement of lead structure **1** to generate inhibitor (+)-**2** (Figure 1), which

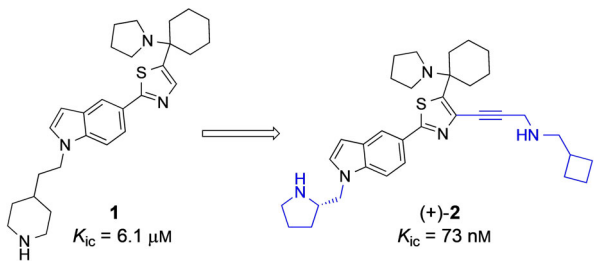

Figure 1. Summary of the inhibitor development presented in this work from lead compound **1**[7] to novel ligand (+)-**2**. The structural differences in (+)-**2** are highlighted in blue. The competitive inhibition constants (K_{ic}) for *T. brucei* TR are indicated.

Table 1. Inhibition of *T. brucei* TR with ligand efficiency (LE) and in vitro activities against *T. brucei rhodesiense* (*T.b.r.*) and mammalian L6 cells by ligands (+)-**2**–**12**. Results of **1**[7] are included for comparison.

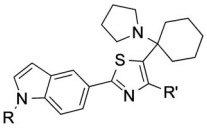

Ligand	R	R′	*T. brucei* TR K_{ic} [μM][a]	LE[b] [kcal mol^{-1}]	*T.b.r.* IC_{50} [μM][c]	L6 IC_{50} [μM][c]
1[7]	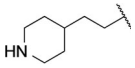		6.1 ± 0.7	0.22	2.0	11.6
(+)-**2**		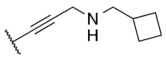	0.073 ± 0.009	0.24	0.12	2.4
(+)-**3**		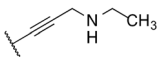	0.24 ± 0.03	0.25	1.56	2.6
(+)-**4**			2.1 ± 0.2	0.25	0.85	3.4
5	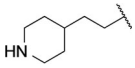	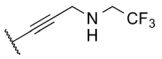	1.5 ± 0.1	0.19	0.05	3.3
6	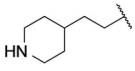	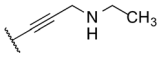	0.78 ± 0.05	0.21	0.78	2.6
7	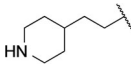	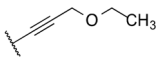	3.5 ± 0.3	0.19	0.14	2.1
8	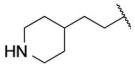	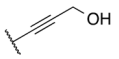	4.3 ± 0.3	0.20	4.20	53.2
9		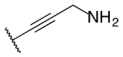	3.9 ± 0.7	0.26	0.75	6.6
10		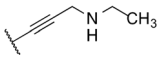	2.8 ± 0.2	0.25	0.70	12.3
11		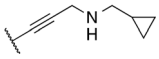	0.80 ± 0.09	0.25	0.18	3.7
12		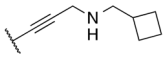	0.41 ± 0.05	0.25	0.61	3.6

[a] At least two different inhibitor concentrations measured. [b] Ligand efficiency = $-RT\ln(K_{ic})$/(number of non-hydrogen atoms), with R = 1.987 kcal K^{-1} mol^{-1} and T = 300 K. [c] Values are the means of two independent assays; individual values vary by less than a factor of 2.

displays a significant, 84-fold enhancement in affinity for *T. brucei* TR resulting in a K_{ic} value of 73 nM. This represents, to the best of our knowledge, the strongest competitive inhibitor of this enzyme reported to date.[2a,3b,5d] The remarkable potency increase was achieved through two major structural changes, the modification of the substituent on the indole moiety, combined with the introduction onto position 4 of the central thiazole moiety of a propargylic substituent, designed to target a hydrophobic sub-pocket near the catalytic cysteines in the TR active site. To evaluate these structural changes, a set of 11 derivatives ((+)-**2**–**12**, Table 1) was synthesized and tested in on-target and cell-based assays. With the exception of **8** and **9**, the calculated topological polar surface area (TPSA,[10] see Section S4 in the Supporting Information for calculated molecular proprieties (clog$D_{7.4}$, TPSA, and pK_a)) was maintained below 80 Å^2 to enhance the probability of the compounds to cross the blood–brain barrier and be active in combatting the central nervous system stage of HAT.[11] For crossing the blood–brain barrier, however, the molecular weights of the ligands between 405 and 545 g mol^{-1} might become limiting (Table S4 in the Supporting Information). Furthermore, co-crystallization of three derivatives with *T. brucei* TR elucidated the binding mode of this class of ligands and revealed a very new direction for further inhibitor improvement.

The strategy employed for the synthesis of ligands (+)-**2**–**12** (see Section S10 in the Supporting Information) is exemplified by the preparation of (+)-**2** starting from intermediate **13** (Scheme 1; see Scheme S4 in the Supporting Information for the synthesis of **13**). A halogen-exchange reaction proved necessary to obtain iodide **14**, which is more reactive towards cross-coupling reactions.[12] Subsequent TIPS-deprotection with KOH provided **15** in 95% yield,[13] which was coupled with tosylated 2-methylpyrrolidine derivative (−)-**16** by nucleophilic substitution,[14] leading to iodide (−)-**17**. Sonogashira cross-coupling[15] was used to introduce the Boc-protected propargylic vector **18**,[16] giving (−)-**19**, which upon Boc-deprotection under basic conditions afforded (+)-**2**.[14] We also investigated heteroalicyclic and aryl vectors as alternatives to the lean propargylic linker but these derivatives proved either synthetically inaccessible or displayed conformational issues in the modeling that would result in a predicted decrease in binding affinity.

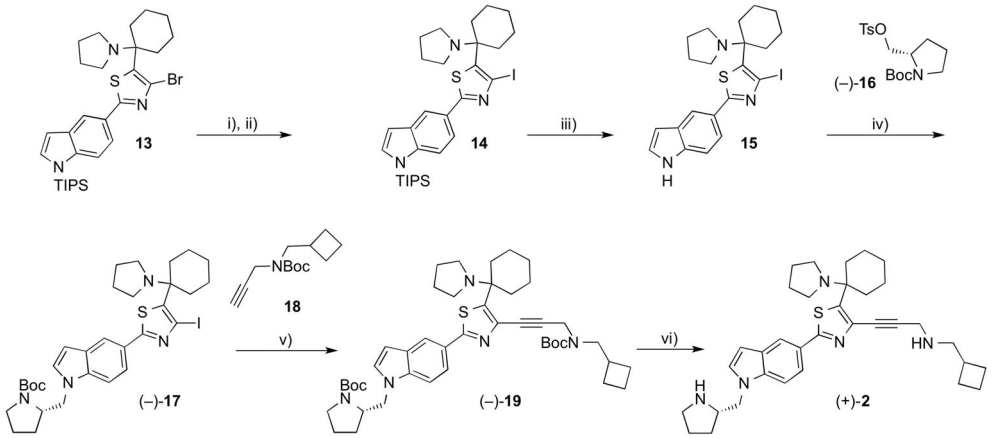

Scheme 1. Synthesis of ligand (+)-**2**. Reagents and conditions: i) *n*BuLi, THF, −78 °C, 15 min; ii) I_2, THF, −78 °C, 25 min, 72%; iii) KOH, THF/MeOH, 25 °C, 15 h, 95%; iv) (−)-**16**, NaH, DMF, 0 °C to 25 °C, 25 h, 50%; v) **18**, $[PdCl_2(PPh_3)_2]$, CuI, Et_3N, 80 °C, 15 h, 48%; vi) TMSOTf, 2,6-lutidine, CH_2Cl_2, 25 °C, 13 h, 76%. TIPS = triisopropylsilyl, THF = tetrahydrofuran, Boc = *tert*-butoxycarbonyl, Ts = *p*-toluenesulfonyl, DMF = *N*,*N*-dimethylformamide, TMSOTf = trimethylsilyl trifluoromethanesulfonate.

Ligands (+)-**2**–**12** were tested in enzymatic assays against *T. brucei* TR (see Section S3 in the Supporting Information for experimental details).[7,17] All ligands inhibited TR through a competitive mechanism (see Figure S4 in the Supporting Information for the Lineweaver–Burk plot of (+)-**2**), with a largely improved affinity, compared to lead compound **1**. The improved affinity does not correlate to a significant improvement of the ligand efficiency (LE) which remains below 0.30 kcal mol^{-1}. Five of the inhibitors displayed K_{ic} values in the sub-micromolar range (Table 1). The structure–activity relationship (SAR) indicated that the improved indole N-substituent provides about a 3-fold gain in affinity ((+)-**3** and (+)-**4** vs. **6** and **1**, respectively). Variation of the propargylic vector revealed that a hydrogen bond donor significantly increases the potency compared to a hydrogen-bond acceptor (**6** vs. **7**). Furthermore, an ethyl group on the propargylic amine provides more potent inhibition than a 2,2,2-trifluoroethyl group (**6** vs. **5**). In compound **6**, the basic propargyl amine is most probably protonated (calculated pK_a value: 10.6, see Table S2 in the Supporting Information), whereas the 2,2,2-trifluoroethyl amine in **5** is expected to be neutral at physiological pH (calculated pK_a value: 5.4).[18] The potency nicely correlates with the size of the propargylic alkyl groups (**9**–**12**), with a 9.5-fold improvement from unsubstituted propargylic amine **9** (K_{ic} = 3.9 μM) to the larger cyclobutyl derivative **12** (K_{ic} = 0.41 μM).

The in vitro activities of (+)-**2**–**12** were studied against *T. brucei rhodesiense*, *T. cruzi*, and *Leishmania* (*L.*) *donovani*, the causative agents of HAT, Chagas' disease, and leishmaniasis, respectively, as well as the malarial parasite *Plasmodium* (*P.*) *falciparum*, and mammalian L6 cells (Table 1 and Table S3 in the Supporting Information). Most ligands showed IC_{50} values (half-maximal inhibitory concentration) against *T. brucei rhodesiense* (*T.b.r.*) in the sub-micromolar range and in the single-digit micromolar range against *T. cruzi*, while being mostly inactive towards *L. donovani*. The activity against *T. cruzi* is probably partially influenced by the cytotoxicity against the host cells, whereas the results against *L. donovani* are likely due to the low concentration of uncharged species at the pH (5.4) of the culture medium, which leads to a very limited cell permeation. Compound **5** was the most active derivative of the series against *T. brucei rhodesiense* with an IC_{50} value of 50 nM, corresponding to a 40-fold improvement compared to **1**, whereas the strongest inhibitor of *T. brucei* TR, (+)-**2**, displayed an IC_{50} value of 120 nM. Additionally, most of the compounds inhibited the proliferation of *P. falciparum* with IC_{50} values in the middle-to-low nanomolar range. This high cell-based inhibition of the malarial parasite has already been observed previously and hints at the inhibition of additional targets, as *P. falciparum* does not possess TR.[5a–c,7,19] Correlation of on-target and cell-based assay results is not straightforward, potentially being caused by these additional targets and differences in cell permeation.

Measurements of the parallel artificial membrane permeation (PAMPA)[20] scores on selected ligands showed that potentially triply positively charged, highly polar ligands displayed low permeation constants Pe, while the permeation improved when one of the protonatable centers was absent resulting in medium-to-high permeation (Section S6 in the Supporting Information for experimental details and results). Conversely, the increased polarity provided improved metabolic stability in microsomal stability assays with human, mouse, and rat microsomes, with (+)-**3** and **6** showing low intrinsic clearance (Cl_{int} < 10 μL min^{-1} mg^{-1}) in human microsomes (Section S7 in the Supporting Information for experimental details and results).[21]

All ligands showed low-to-moderate selectivity against mammalian L6 myoblast cells with selectivity indices (S.I. = L6/*T.b.r.*) up to 68 for **5** (Table 1 and Table S3 in the Supporting Information). Cytotoxicity might arise from alternative inhibition targets in mammalian cells. Interestingly and in accordance with our previous results,[5c,7] the basic, most probably protonated indole N-substituents of ligands **1**–**8** vastly improved selectivity against hGR, with no measurable inhibition of the human enzyme. The unsubstituted indoles **9**–**12** displayed slight binding affinity towards hGR (Table S1 in the Supporting Informa-

tion). Ligand **12** was chosen for a detailed kinetic analysis and was found to inhibit hGR noncompetitively with a K_i value of 83 μM (Figure S3 in the Supporting Information for Lineweaver–Burk plot), corresponding to a selectivity of TR over hGR above 200-fold for **12**.

Co-crystal structures of ligands (+)-**2** (PDB ID: 6OEZ, 2.5 Å resolution), (+)-**4** (PDB ID: 6OEY, 2.1 Å resolution), and **5** (PDB ID: 6OEX, 2.1 Å resolution) in complex with *T. brucei* TR were determined (see Section S8 in the Supporting Information for additional information). Analysis of the binding modes provides insight into the observed on-target activities. The two active sites of the homodimeric enzyme, both protein residues and ligands, show distinct differences in the definition and quality of the respective electron densities as well as in their temperature factors. Assignment of active sites A and B is consistent with previous publications.[5c,7] The discussion is mainly focused on active site B with its higher quality electron density.

The indolyl-thiazole core of the ligands binds to the hydrophobic wall of the mepacrine binding site in TR, as previously observed, and its interactions are not further discussed here.[5c,7] The improved indole N-substituent increases the potency of the ligand by positioning the protonated nitrogen of the pyrrolidine in closer proximity to the carboxylate of Asp116 (d(N···O_{Asp116}) = 3.5 and 4.1 Å for (+)-**2** (Figure 2a) and (+)-**4**, respectively (Figure S8, Supporting Information)) allowing for efficient Coulombic interactions. The newly introduced substituent on the thiazole moiety in (+)-**2** establishes in active site B a weak, H-bonding-type electrostatic interaction between the probably protonated propargylic amine and the hydroxyl oxygen of Tyr110 (d(N···O_{Tyr110}) = 4.1 Å), hydrophobic interactions with the residues Val53, Val58, Ile106, and Leu339′[22] (d(C···C) = 3.6–4.5 Å), and a contact with C(2) of the imidazole of His461′ (d(C···$C_{His461'}$) = 3.7 Å) (Figure 2). Whereas, in active site A, the cyclobutylmethyl moiety does not point directly towards the described hydrophobic sub-pocket, but rather to-

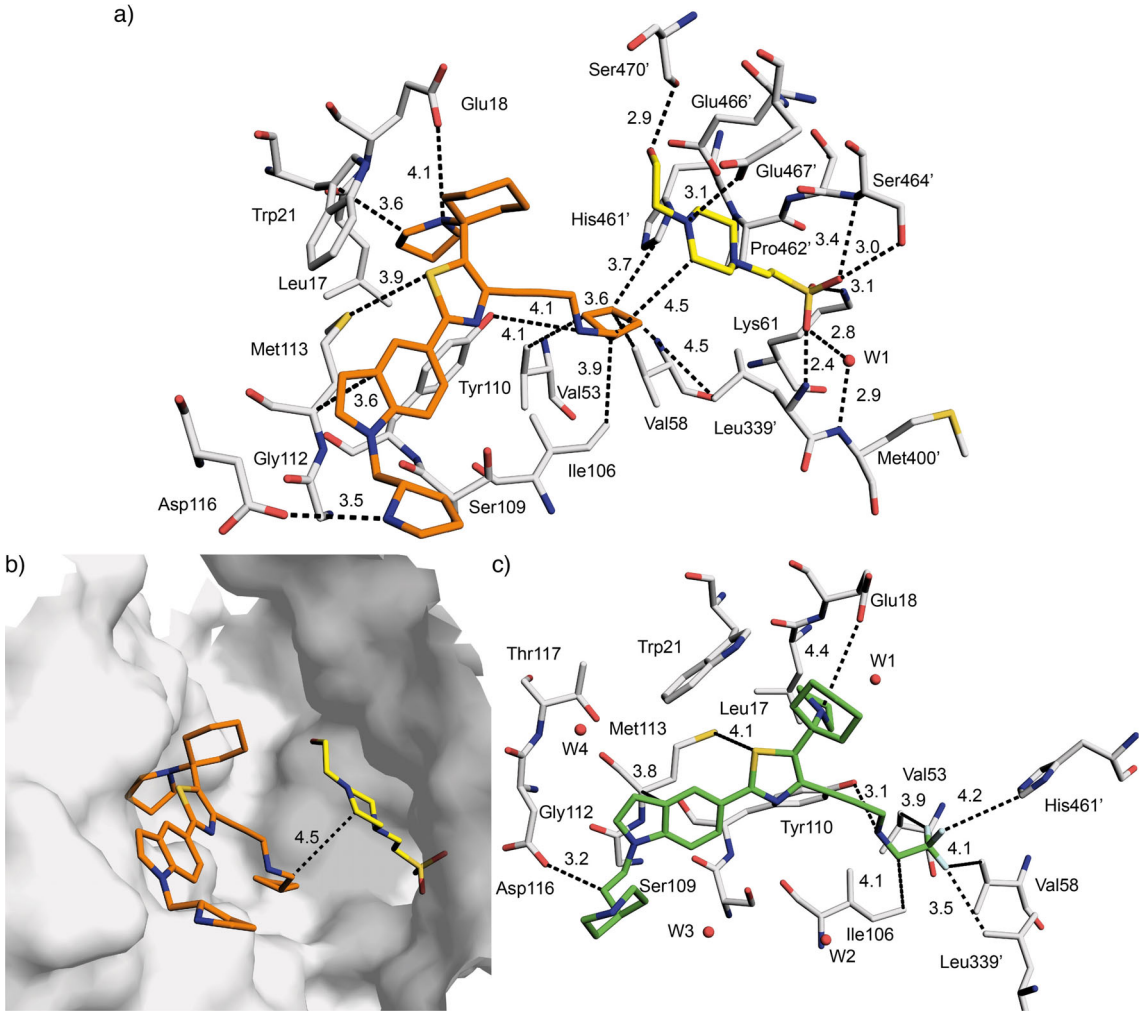

Figure 2. Molecular interactions of ligands (+)-**2**, **5**, and HEPES with *T. brucei* TR. a) The binding mode of (+)-**2** and the HEPES molecule in active site B (PDB ID: 6OEZ, 2.5 Å resolution), close-ups of individual binding modes are represented in Figures S5 and S7 in the Supporting Information. Water molecule W1 involved in the binding of HEPES is marked as a red sphere. Phe396′ and Pro398′ are omitted for clarity. b) Overview of the active site B (PDB ID: 6OEZ, 2.5 Å resolution) showing the close proximity of ligand (+)-**2** to the HEPES molecule. Monomer A is depicted in darker grey and monomer B in lighter grey. c) The binding mode of **5** in active site B (PDB ID: 6OEX, 2.1 Å resolution); the water molecules at distances < 5 Å from **5** are shown as red spheres. Color code: C_{TR} gray, $C_{(+)\text{-}2}$ orange, C_5 green, C_{HEPES} yellow, F white, N blue, O red, S yellow. Distances are given in Å and indicated by dashed lines. All crystallographic representations were prepared using PyMOL.[23]

wards the side chains of Thr335 and Ile339, with additional close C–H···π interactions with His461′ (Figures S5 and S6 in the Supporting Information). In the structure of **5**, similar interactions with Tyr110 (d(N···O_{Tyr110}) = 3.1 Å) and the hydrophobic sub-pocket (Val53, Val58, and Ile106) are observed (Figure 2c). Overall, the observed binding mode of (+)-**2** in active site B of the X-ray co-crystal structure corresponds to the one predicted in our design (see Section S2 in the Supporting Information).

The origin of the significantly weaker TR binding of **5** (K_i value: 1.5 μM) compared to (+)-**2** (73 nM) remains unclear after structural analysis. The most probably protonated propargyl amine of (+)-**2** forms a longer, much weaker H bond (4.1 Å) to the phenolic O-atom of Tyr110 than the neutral amine in **5** (3.1 Å). Also, the CF_3 group does not engage in repulsive electrostatic interactions[24] but rather accommodates well in a hydrophobic surrounding shaped by Ile106, Leu339′, Val58, Val53, and His461′.[24]

In previously published structures,[5c,7] a large unexplained density had been observed close to the entrance to the Z-site[25] in active site B. The higher resolution of our present co-crystal structures allows to assign this density to a HEPES (2-[4-(2-hydroxyethyl)piperazin-1-yl]ethanesulfonic acid) buffer molecule (Figure 2 and Figures S7–9 in the Supporting Information). This observation highlights that further opportunities for ligand-protein interactions are available in the wide TR active site. It provides inspiration for the structure-based development of even stronger inhibitors combining the interactions established by current ligands and the HEPES molecule, for example, by extending the propargylic vector to also displace the buffer molecule (see Figure S7, Supporting Information, for a detailed representation of its binding mode). In the structures of (+)-**2** and **5**, the closest distances between the HEPES molecule and the propargylic vector of the ligands in active site B are only 4.5 and 3.9 Å, respectively. In the complex with (+)-**4** an additional ligand molecule is found stacking to the main binding ligand in active site B (Figure S8 in the Supporting Information), as already observed in other co-crystal structures of TR inhibitors.[26]

In conclusion, we investigated two main structural modifications of lead compound **1**, namely the improvement of the indole N-substituent and the introduction of a lean propargylic substituent in position 4 of the thiazole moiety. These modifications provided a remarkable enhancement of the binding affinity towards *T. brucei* TR with five inhibitors showing K_{ic} values in the sub-micromolar range. The most potent ligand of the series (+)-**2** resulted in a K_{ic} value of 73 nM. To the best of our knowledge, it is the strongest competitive inhibitor of this enzyme reported to date. Only a noncompetitive polyamine-based ligand reported by Chitkul and Bradley had a similar potency, with a K_i value for *T. cruzi* TR of 76 nM; this ligand has not been tested on cells.[27] Our new ligands showed strong in vitro activities with IC_{50} values for (+)-**2** and **5** of 120 nM and 50 nM, respectively. Their binding modes were elucidated from co-crystal structures which also revealed the complexation of a HEPES buffer molecule in close proximity. This new structural insight paves the way for the structure-based design of the next-generation inhibitors with low nanomolar activities for future in vivo studies. We propose a further extension of the propargylic vector to replace the buffer molecule.

Acknowledgements

The authors thank the ETH Research Council (ETH-01 13-2) for support. Research at the University of Heidelberg was supported by the Deutsche Forschungsgemeinschaft (DFG KR 1242/8-1) and at the University of Toronto by the Natural Sciences and Engineering Research Council of Canada (RGPIN-2015-04877) and the Canadian Research Chairs Program. We thank Dr. Massimiliano Donzelli and Björn Wagner from F. Hoffmann-La Roche Ltd for PAMPA and microsomal stability measurements. We are grateful to Dr. Bruno Bernet (ETH) for proofreading the Experimental Section, and Dr. Cédric Schaack (ETH) for proofreading the entire manuscript and helpful discussions. Monica Cal (Swiss TPH), Romina Rocchetti (Swiss TPH) and Sonja Keller-Märki (Swiss TPH) helped with the parasite assays. We thank Natalie Dirdjaja (BZH) for the preparation of trypanothione disulfide and TR enzyme, and G. Prive (UHN) for use of diffraction equipment. Use of the IMCA-CAT beamline 17-ID at the Advanced Photon Source was supported by the companies of the Industrial Macromolecular Crystallography Association through a contract with Hauptman-Woodward Medical Research Institute. This research used resources of the Advanced Photon Source, a U.S. Department of Energy (DOE) Office of Science User Facility operated for the DOE Office of Science by Argonne National Laboratory under Contract No. DE-AC02-06CH11357.

Conflict of interest

The authors declare no conflict of interest.

Keywords: antiprotozoal agents · co-crystals · molecular recognition · neglected diseases · X-ray diffraction

[1] a) K. Stuart, R. Brun, S. Croft, A. Fairlamb, R. E. Gürtler, J. McKerrow, S. Reed, R. Tarleton, *J. Clin. Invest.* **2008**, *118*, 1301 – 1310; b) M. P. Barrett, S. L. Croft, *Br. Med. Bull.* **2012**, *104*, 175 – 196; c) GBD 2015 Disease and Injury Incidence and Prevalence Collaborators, *Lancet* **2016**, *388*, 1545 – 1602, https://doi.org/10.1016/S0140-6736(16)31678-6; d) *Fourth WHO Report on Neglected Tropical Diseases*, World Health Organization, **2017**, ISBN 978-992-4-156544-8.

[2] a) L. S. C. Bernardes, C. L. Zani, I. Carvalho, *Curr. Med. Chem.* **2013**, *20*, 2673 – 2696; b) A. S. Nagle, S. Khare, A. B. Kumar, F. Supek, A. Buchynskyy, C. J. N. Mathison, N. K. Chennamaneni, N. Pendem, F. S. Buckner, M. H. Gelb, V. Molteni, *Chem. Rev.* **2014**, *114*, 11305 – 11347.

[3] a) A. H. Fairlamb, A. Cerami, *Annu. Rev. Microbiol.* **1992**, *46*, 695 – 729; b) R. L. Krauth-Siegel, H. Bauer, R. H. Schirmer, *Angew. Chem. Int. Ed.* **2005**, *44*, 690 – 715; *Angew. Chem.* **2005**, *117*, 698 – 724.

[4] a) S. L. Shames, A. H. Fairlamb, A. Cerami, C. T. Walsh, *Biochemistry* **1986**, *25*, 3519 – 3526; b) R. L. Krauth-Siegel, B. Enders, G. B. Henderson, A. H. Fairlamb, R. H. Schirmer, *Eur. J. Biochem.* **1987**, *164*, 123 – 128.

[5] a) C. Eberle, J. A. Burkhard, B. Stump, M. Kaiser, R. Brun, R. L. Krauth-Siegel, F. Diederich, *ChemMedChem* **2009**, *4*, 2034 – 2044; b) C. Eberle, B. S. Lauber, D. Fankhauser, M. Kaiser, R. Brun, R. L. Krauth-Siegel, F. Diederich, *ChemMedChem* **2011**, *6*, 292 – 301; c) E. Persch, S. Bryson, N. K. Todoroff, C. Eberle, J. Thelemann, N. Dirdjaja, M. Kaiser, M. Weber, H. Derbani, R. Brun, G. Schneider, E. F. Pai, R. L. Krauth-Siegel, F. Diederich,

ChemMedChem **2014**, *9*, 1880 – 1891; d) A. E. Leroux, R. L. Krauth-Siegel, *Mol. Biochem. Parasitol.* **2016**, *206*, 67 – 74.
[6] S. Krieger, W. Schwarz, M. R. Ariyanayagam, A. H. Fairlamb, R. L. Krauth-Siegel, C. Clayton, *Mol. Microbiol.* **2002**, *35*, 542 – 552.
[7] R. De Gasparo, E. Brodbeck-Persch, S. Bryson, N. B. Hentzen, M. Kaiser, E. F. Pai, R. L. Krauth-Siegel, F. Diederich, *ChemMedChem* **2018**, *13*, 957 – 967.
[8] a) J. L. Richardson, I. R. E. Nett, D. C. Jones, M. H. Abdille, I. H. Gilbert, A. H. Fairlamb, *ChemMedChem* **2009**, *4*, 1333 – 1340; b) S. Patterson, D. C. Jones, E. J. Shanks, J. A. Frearson, I. H. Gilbert, P. G. Wyatt, A. H. Fairlamb, *ChemMedChem* **2009**, *4*, 1341 – 1353.
[9] E. M. Jacoby, I. Schlichting, C. B. Lantwin, W. Kabsch, R. L. Krauth-Siegel, *Proteins Struct. Funct. Genet.* **1996**, *24*, 73 – 80.
[10] P. Ertl, B. Rohde, P. Selzer, *J. Med. Chem.* **2000**, *43*, 3714 – 3717.
[11] K. M. Mahar Doan, J. E. Humphreys, L. O. Webster, S. A. Wring, L. J. Shampine, C. J. Serabjit-Singh, K. K. Adkison, J. W. Polli, *J. Pharmacol. Exp. Ther.* **2002**, *303*, 1029 – 1037.
[12] a) A. Bähr, A. S. Droz, M. Püntener, U. Neidlein, S. Anderson, P. Seiler, F. Diederich, *Helv. Chim. Acta* **1998**, *81*, 1931 – 1963; b) K. Morinaka, T. Ubukata, Y. Yokoyama, *Org. Lett.* **2009**, *11*, 3890 – 3893; c) V. García-López, L. B. Alemany, P.-T. Chiang, J. Sun, P.-L. Chu, A. A. Martí, J. M. Tour, *Tetrahedron* **2017**, *73*, 4864 – 4873.
[13] B. J. Littler, M. A. Miller, C.-H. Hung, R. W. Wagner, D. F. O'Shea, P. D. Boyle, J. S. Lindsey, *J. Org. Chem.* **1999**, *64*, 1391 – 1396.
[14] L. Zhang, M. Su, J. Li, X. Ji, J. Wang, Z. Li, J. Li, H. Liu, *Chem. Biol. Drug Des.* **2013**, *81*, 198 – 207.
[15] K. Sonogashira, *J. Organomet. Chem.* **2002**, *653*, 46 – 49.
[16] H. Yamamura, M. Nonaka, S. Okuno, R. Mitsuhashi, H. Kato, T. Katsu, K. Masuda, K. Tanimoto, H. Tomita, A. Miyagawa, *MedChemComm* **2018**, *9*, 509 – 518.
[17] a) M. C. Jockers-Scherübl, R. H. Schirmer, R. L. Krauth-Siegel, *Eur. J. Biochem.* **1989**, *180*, 267 – 272; b) A. Nordhoff, U. S. Bücheler, D. Werner, R. H. Schirmer, *Biochemistry* **1993**, *32*, 4060 – 4066.
[18] M. Morgenthaler, E. Schweizer, A. Hoffmann-Röder, F. Benini, R. E. Martin, G. Jaeschke, B. Wagner, H. Fischer, S. Bendels, D. Zimmerli, J. Schneider, F. Diederich, M. Kansy, K. Müller, *ChemMedChem* **2007**, *2*, 1100 – 1115.
[19] a) B. Stump, C. Eberle, M. Kaiser, R. Brun, R. L. Krauth-Siegel, F. Diederich, *Org. Biomol. Chem.* **2008**, *6*, 3935 – 3947; b) B. Stump, C. Eberle, W. B. Schweizer, M. Kaiser, R. Brun, R. L. Krauth-Siegel, D. Lentz, F. Diederich, *ChemBioChem* **2009**, *10*, 79 – 83.
[20] a) M. Kansy, F. Senner, K. Gubernator, *J. Med. Chem.* **1998**, *41*, 1007 – 1010; b) S. Winiwarter, N. M. Bonham, F. Ax, A. Hallberg, H. Lennernäs, A. Karlén, *J. Med. Chem.* **1998**, *41*, 4939 – 4949.
[21] L. Di, C. Keefer, D. O. Scott, T. J. Strelevitz, G. Chang, Y.-A. Bi, Y. Lai, J. Duckworth, K. Fenner, M. D. Troutman, R. S. Obach, *Eur. J. Med. Chem.* **2012**, *57*, 441 – 448.
[22] Residues marked with a prime belong to the partner monomer forming the active site in the homodimeric enzyme.
[23] *The PyMOL Molecular Graphics System*, Version 1.8.6.2, Schrödinger LLC, **2018**.
[24] a) K. Müller, C. Fäh, F. Diederich, *Science* **2007**, *317*, 1881 – 1886; b) B. S. Lauber, L. A. Hardegger, A. K. Asraful, B. A. Lund, O. Dumele, M. Harder, B. Kuhn, R. A. Engh, F. Diederich, *Chem. Eur. J.* **2016**, *22*, 211 – 221; c) A. Schwab, B. Illarionov, A. Frank, A. Kunfermann, M. Seet, A. Bacher, M. C. Witschel, M. Fischer, M. Groll, F. Diederich, *ACS Chem. Biol.* **2017**, *12*, 2132 – 2138.
[25] a) A. El-Waer, K. T. Douglas, K. Smith, A. H. Fairlamb, *Anal. Biochem.* **1991**, *198*, 212 – 216; b) J. Garforth, J. H. McKie, R. Jaouhari, T. J. Benson, A. H. Fairlamb, K. T. Douglas, *Amino Acids* **1994**, *6*, 295 – 299.
[26] a) A. Saravanamuthu, T. J. Vickers, C. S. Bond, M. R. Peterson, W. N. Hunter, A. H. Fairlamb, *J. Biol. Chem.* **2004**, *279*, 29493 – 29500; b) P. Baiocco, G. Poce, S. Alfonso, M. Cocozza, G. C. Porretta, G. Colotti, M. Biava, F. Moraca, M. Botta, V. Yardley, A. Fiorillo, A. Lantella, F. Malatesta, A. Ilari, *ChemMedChem* **2013**, *8*, 1175 – 1183; c) F. Saccoliti, G. Angiulli, G. Pupo, L. Pescatori, V. N. Madia, A. Messore, G. Colotti, A. Fiorillo, L. Scipione, M. Gramiccia, T. Di Muccio, R. Di Santo, R. Costi, A. Ilari, *J. Enzyme Inhib. Med. Chem.* **2017**, *32*, 304 – 310.
[27] B. Chitkul, M. Bradley, *Bioorg. Med. Chem. Lett.* **2000**, *10*, 2367 – 2369.

Manuscript received: April 10, 2019
Revised manuscript received: July 3, 2019
Version of record online: ■■ ▮▮, 0000

COMMUNICATION

Potency improvement by rational design: Trypanothione reductase (TR) is a drug target for trypanosomatidae-caused diseases. By optimizing known TR ligands and using structure-based design, a new series of potent TR inhibitors with target and cell-based activities in the middle to upper nanomolar range was developed. X-Ray co-crystal structures confirmed the binding modes and revealed opportunities for a further increase in ligand potency towards in vivo studies.

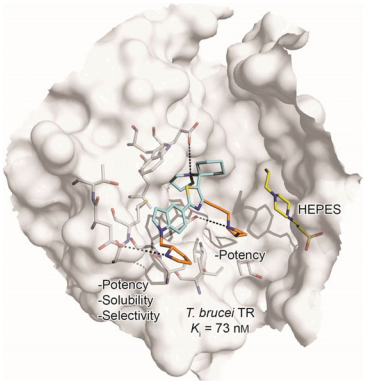

Enzyme Inhibitors

R. De Gasparo, O. Halgas, D. Harangozo, M. Kaiser, E. F. Pai,* R. L. Krauth-Siegel,* F. Diederich**

■■ – ■■

Targeting a Large Active Site: Structure-Based Design of Nanomolar Inhibitors of *Trypanosoma brucei* Trypanothione Reductase